Geophys. J. R. astr. Soc. (1976) **47**, 445–457

Annual variation of the geomagnetic field

S. R. C. Malin *Institute of Geological Sciences, Herstmonceux Castle, Hailsham, Sussex*

A. Mete Işikara *T.C. Istanbul Universitesi, Fen Fakültesi, Jeofizik Kürsüsü, Istanbul, Turkey*

Received 1976 April 15

Summary. Horizontal and vertical intensity data, obtained between 1957.0 and 1961.0 at 69 observatories, are analysed to determine the worldwide distribution of the annual variation of the geomagnetic field. Only data observed near local midnight are used, to avoid the small, but significant contamination from Sq. Over most of the world the variation is found to be small, with a clear dependence on latitude, but near the poles it is larger and more erratic. The non-polar variation is subjected to spherical harmonic analysis and separated into parts of internal and external origin. The polar variations are shown to be consistent with a north–south oscillation of the mean position of the auroral electrojets during the year. It is suggested that, with the exception of the polar effect, the annual variation is not due to ionospheric currents (as was hitherto believed), but results from an annual variation in the latitude of the ring current.

1 Introduction

The annual variation considered here is the variation of the geomagnetic field with a period of one cycle per yr. Some authors include additional terms, particularly the dominant semi-annual harmonic, in their definition of annual variation, but these are excluded from the present study.

The annual term is of interest on two counts. Firstly, it is the lowest frequency of geomagnetic variation that can be reliably separated into parts of internal and external origin, for subsequent use in determining the conductivity of the mantle. The low-frequency end of the spectrum is of particular importance for determining the deeper conductivity. In principle, the 11-yr sunspot cycle should provide a point at even lower frequency, but no convincing results have yet been obtained. Secondly, if the interpretation of Vestine (1954) is correct – it receives support from McIntosh (1959), Currie (1966) and Banks (1969) – the annual variation results from dynamo action in the ionosphere, and hence presents a valuable opportunity for studying ionospheric dynamo characteristics at a particularly low frequency.

The earlier investigations of Lloyd (1874), Schwalbe (1898, 1899), Cynk (1939) and Vestine *et al.* (1947) were hampered by the lack of adequate baseline control at most of the observatories. To reveal adequately an annual variation with an amplitude of only a few nT requires baseline control of a very high standard, which was probably beyond the capability of most of the absolute instruments in use at observatories before 1940. The subsequent development of more accurate instruments (particularly for the measurement of the vertical component) and the gradual acquisition of these by observatories has produced a significant improvement in the absolute values of observatory data. This can readily be seen by examining the scatter in plots of first-differences of observatory annual mean values, such as are used in secular variation studies. To alleviate the problem of baseline control, Cynk (1939) and Vestine *et al.* (1947) examined differences between quiet-day and disturbed-day data. They showed that the annual term was closely sinusoidal in character, indicating that it is a genuine harmonic and not merely noise, and delineated the general features of its global distribution; in particular, the increased amplitude in the vertical component at high latitude. Vestine *et al.* (1947) also attempted a spherical harmonic analysis, but were unable to obtain a significant result.

More recently Currie (1966) and Banks (1969) have investigated the amplitude and phase of the annual variation using spectral analysis techniques. They confirm that there is, indeed, a well-defined line with a frequency of one cycle per yr. They also showed that the distribution of amplitude and phase is consistent with a P_2^0 distribution of magnetic potential, rather than P_1^0, which is the usual pattern associated with disturbance phenomena. Vestine (1954) had previously interpreted the P_2^0 pattern as that associated with electric currents in the ionosphere generated by winds that blow from north to south during northern summer, and south to north in winter. This interpretation was accepted by Currie (1966) after a further examination of the meteorological evidence, and by Banks (1969). Banks also made a spherical harmonic analysis of his own, very limited, data set, and of Currie's more extensive data, on the assumption that they could be represented by P_2^0 only. However, he remarks that 'P_2^0 is probably far from being an adequate representation of its spatial behaviour' (Banks 1972).

Banks and Currie analysed data meaned over all solar hours, so their annual terms include a contribution from the daily variation. The quiet daily variation (Sq), resulting from dynamo action in the ionosphere, may be assumed to have a zero value near local midnight, since the conductivity of the dynamo region falls nearly to zero at this time. However, the mean value of Sq is not zero, so the daily mean will differ from the midnight (baseline) value. Gupta & Malin (1972) have shown that the range of Sq doubles from winter to summer, and it is reasonable to expect a similar change in the departure of the daily mean value from the midnight value, leading to an apparent annual term that is merely a modulation of the diurnal amplitude. At one time Currie believed this mechanism to account for the whole of the annual variation, but later withdrew this suggestion (Currie 1974). This Sq effect is present in the data of Currie and Banks, and in most of the data of Vestine *et al.* (1947), but was removed by Cynk (1939) in the process of subtracting quiet day from disturbed day means.

In the present study we estimate the importance of the Sq effect, and then examine the global distribution of the annual term after removal of this effect. A more extensive and uniform data set is used than hitherto, giving a more detailed picture of the phenomenon and permitting a reliable separation into parts of internal and external origin.

2 Preliminary investigation

As a preliminary to the main analysis, horizontal (H) and vertical intensity (Z) data were examined to decide the best way of extracting the annual term, and to reveal some of its characteristics. The data were from three stations: one northern (Hartland: 51°.0 N, 355°.5 E), one southern (Hermanus: 34°.4 S, 19°.2 E) and one equatorial (Huancayo: 12°.0 S, 284°.7 E). Varying intervals of monthly mean data were considered, derived from various combinations of all days, quiet days, disturbed days; daily means, night-time means (5 hours centred on local midnight) and midnight values.

It was found that the annual term could be reliably determined from a few years of suitably filtered monthly means, that it was enhanced in amplitude at sunspot maximum and that there were small but significant differences between the results from night-time, quiet-day and all-day mean data. This agrees with the findings of van Wijk (1953) for Hermanus. Accordingly, it was decided to analyse data obtained during the sunspot maximum period 1957.0–1961.0, when a particularly large number of well-distributed magnetic observatories was operating. The remainder of this note refers to data from that interval.

The method of filtering, adopted after some experimentation, was as follows. High-frequency contributions were removed by taking 3-month running means.

$$S_i = 1.11(m_{i-1} + m_i + m_{i+1})/3. \tag{1}$$

Here, m_i denotes the ith monthly mean, and the factor 1.11 compensates for the reduction in amplitude of an annual term, resulting from the smoothing process. Low frequencies and the dominant semi-annual term were removed by taking second differences of values separated by six months:

$$f_j = -(S_{j+6} - 2S_j + S_{j-6})/4. \tag{2}$$

The annual variation may be clearly seen in the filtered monthly values, f_j (see, e.g. Fig. 2). Assuming the annual variation (here denoted A_1 to distinguish it from the semi-annual variation, A_2) to be of the form

$$A_1 = a \sin t + b \cos t = c \cos(t + \theta), \tag{3}$$

and ignoring the variation in the length of a month, we determine the harmonic constants a, b and their standard deviations by least squares analysis of the f_j values for each station. Here t denotes time measured from January 1.0 and increasing by 2π in the course of a year. From a, b we may deduce c and θ, the amplitude and phase constant of A_1.

Values of c, θ for the three pilot stations are given in Table 1 for standard monthly means (M), monthly means of all midnight values (N) and monthly means of midnight values for the five International Quiet Days only (Q). Also given are the vector probable errors (vpe) which are deduced from the standard deviations of a, b, and represent the radius of the circle that would contain the end points of half the experimental determinations of c, θ plotted on a harmonic dial. For the difference between two measures of c, θ to be significant at the

Table 1. Amplitude, vpe and phase of the annual term in data from three stations.

		M data			N data			Q data		
Station	Element	Amp. (nT)	vpe (nT)	Phase (deg)	Amp. (nT)	vpe (nT)	Phase (deg)	Amp. (nT)	vpe (nT)	Phase (deg)
Hartland	*H*	6.16	0.47	215	7.84	0.47	198	5.93	0.59	201
Huancayo	*H*	6.46	0.85	12	3.56	0.99	34	3.38	1.17	59
Hermanus	*H*	8.70	0.75	16	10.07	0.67	13	8.61	1.07	1
Hartland	*Z*	3.21	0.40	42	3.28	0.39	17	2.00	0.46	63
Huancayo	*Z*	5.64	0.31	198	7.21	0.29	187	6.74	0.23	188
Hermanus	*Z*	1.55	0.36	330	1.20	0.44	332	0.82	0.68	283

5 per cent level, their vector difference must exceed 1.67 times the root of the sum of the squares of their vpe's (Leaton, Malin & Finch 1962). We assume that the magnetic variations of external origin are the sum of Sq, SD (the disturbance daily variation, mainly due to currents associated with particles precipitated into the polar ionosphere) and D_{st} (the storm-time variation, resulting from a torus of charged particles parallel to the magnetic equator at a distance of a few Earth radii – the ring current). Then the **M** data contain Sq, SD and D_{st}, the **N** data contain D_{st} and the midnight part of SD, and the **Q** data contain only D_{st}, though at a reduced level.

The data of Table 1 show that, for each station, the **M**, **N** and **Q** results are essentially similar, suggesting that the main contribution to the annual variation comes from the ring current. However, the majority of the differences between **M** and **N** are significant, indicating a small but significant annual term from Sq. No obvious pattern of its distribution emerges, but this is hardly surprising from only three stations. Similar small but significant differences are found between **N** and **Q** with the amplitudes for **Q** less than those for **N** in all cases but one. One might expect the exclusion of SD to have a greater effect in the auroral regions than at the latitudes of our test stations, and it is found that for Godhavn (69°.2 N) the amplitude of $A_1(H)$ is reduced from (35 ± 1) nT for **N**, to (20 ± 1) nT for **Q** data. However, it is not clear how much of this reduction is due to the removal of SD, and how much is due to the reduction of the ring-current effect during quiet days.

If the quality of a determination may be measured by the ratio of its amplitude to its vpe, we find that, in four of the six cases, the **N** results are better than those from **M**, and that all but one of the **N** results are better than those from **Q** data.

3 Data and analysis

From the preliminary investigation we conclude that a good determination of A_1, free from contamination by Sq, may be obtained from monthly means of H and Z data based on the mean hourly values nearest to local midnight for the interval 1957.0–1961.0.

Such data for a worldwide distribution of observatories (those shown in Fig. 1) were obtained from the observatory year books and from the files of World Digital Data Centre C1. They were analysed for a and b as described in Section 2. Where values appeared anomalous, or the residuals from f_j appeared excessive, the original data were re-examined for errors or discontinuities. In most cases there was a simple explanation, such as an unnoticed change of tabular base, or a transcription error. In a few cases it was clear that the observatory instrumentation was not adequate to maintain a stable baseline, and such stations were rejected. For 15 stations, data were available for only the 18 months of the International Geophysical Year, and thus yielded only four values of f_j from which to determine a and b. For these stations a more economical (though less efficient) filter was used in which the mean and a linear approximation to secular change was removed from S_i, but no attempt was made to remove the semi-annual variation (A_2). The lower quality of the results from these stations is reflected in their relatively large standard deviations.

The final values of a, b and their standard deviations are given in Table 2, in decreasing order of geographical latitude. A representative selection of the values of f_j from which they were derived is plotted in Fig. 2, which illustrates how closely the pattern is repeated from year to year, and the extent of the departures from a sine wave.

We would not expect A_1 to have much longitudinal dependence, since the internal currents induced by a variation of this frequency will not be appreciably affected by near-surface conductivity anomalies, such as the oceans. The main factor controlling the distribution of A_1 is likely to be the configuration of the main magnetic field. Fig. 3 shows

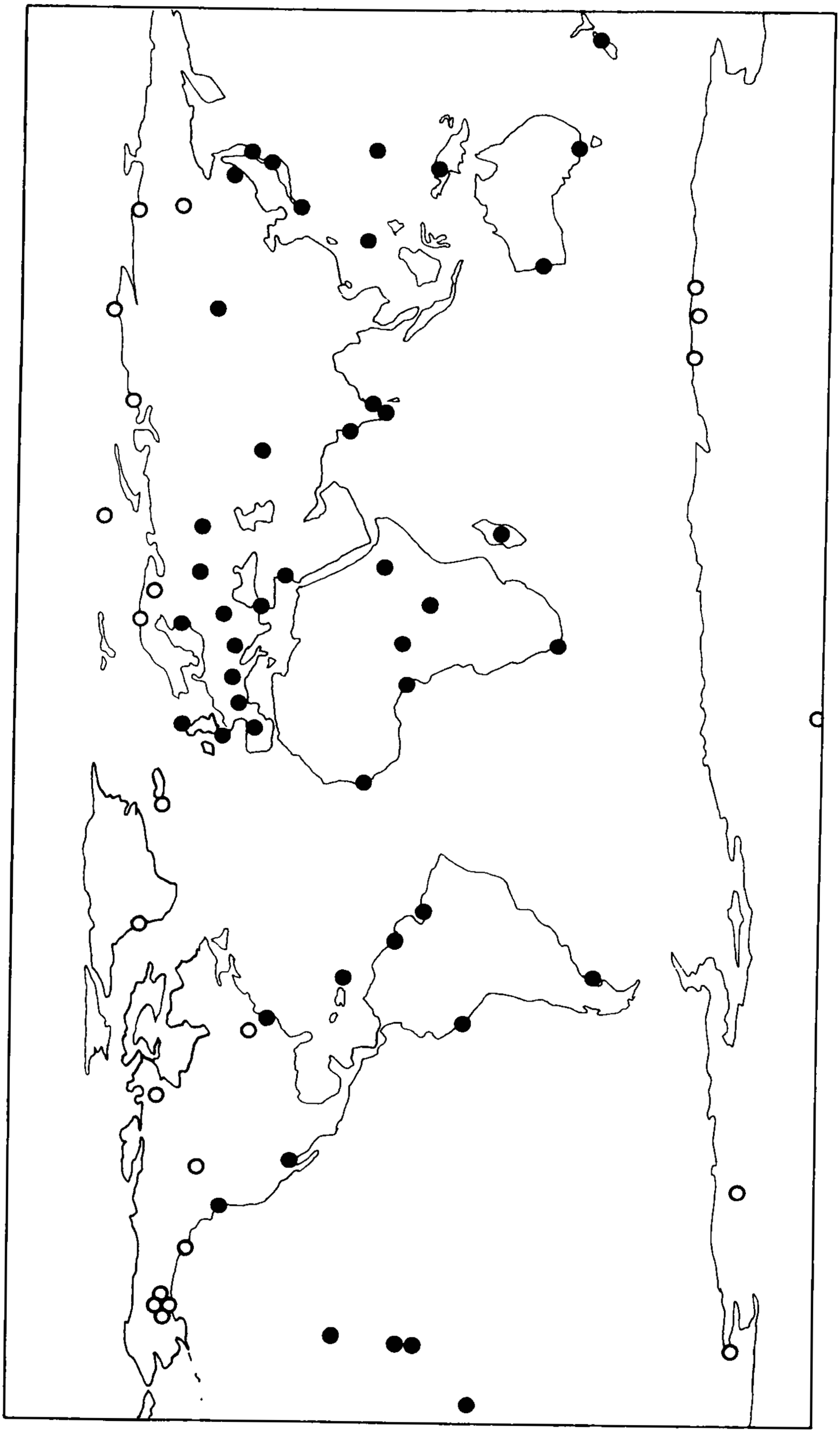

Figure 1. Distribution of observatories whose data were analysed. Those marked by open circles were omitted from the spherical harmonic analysis.

Table 2. Harmonic constants of the annual term in units of 0.01 nT.

Station	Latitude (deg)	E. longitude (deg)	H a		H b		Z a		Z b	
Tikhaya Bay	80.3	52.8	256	±319	−1445	±319	−424	±159	−97	±159
Chelyuskin	77.7	104.3	−79	166	−1880	197	1364	120	2977	144
Dixon	73.5	80.6	−1326	197	−2166	235	907	113	1127	135
Tixi	71.6	129.0	685	126	−4777	150	−2371	254	−211	302
Tromso	69.7	19.0	−1057	312	1469	328	872	250	−2194	263
Godhavn	69.2	306.5	751	71	−3422	75	−198	169	759	178
Sodankyla	67.4	26.6	−452	452	1713	476	−65	129	−271	136
College	64.9	212.2	1278	210	−1203	221	−811	89	−942	94
Baker Lake	64.3	264.0	441	110	−2633	116	187	260	1661	273
Leirvogur	64.2	338.3	−397	379	2733	404	−523	153	−2171	163
Big Delta	64.0	214.2	414	246	−161	246	−548	208	7	208
Healy	63.8	211.0	42	431	−232	431	−30	205	−29	205
Yakutsk	62.0	129.7	−514	203	−1625	203	1401	111	348	111
Anchorage	61.2	210.1	1006	267	−327	267	1208	155	1751	155
Nurmijarvi	60.5	24.7	183	52	−228	55	−244	106	437	112
Lerwick	60.1	358.8	177	137	538	144	−366	146	886	154
Sitka	57.1	224.7	847	118	−676	124	366	130	369	136
Kazan	55.8	48.9	−9	136	185	136	−423	180	−404	180
Moscow	55.5	37.3	299	140	−412	140	−379	89	−237	89
Meanock	54.6	246.7	635	324	114	341	1552	169	571	178
Irkutsk	52.5	104.0	21	96	−986	96	613	138	−849	138
Hartland	51.0	355.5	246	39	−744	41	−94	32	314	34
Lvov	49.9	23.8	142	143	−613	143	43	118	−187	118
Victoria	48.5	236.6	23	93	−775	99	253	131	99	140
Tihany	46.9	17.9	−27	49	−751	51	−154	32	−81	34
Furstenfeldbruck	48.2	11.3	293	35	−693	37	14	60	173	63
Chambon la Forêt	48.0	2.3	101	46	−1028	49	−538	78	−241	82
Yuzhno Sakhalinsk	47.0	142.7	−171	147	−981	147	337	109	−145	109
Memambetsu	43.9	144.2	290	52	−569	54	38	41	−246	44
Agincourt	43.8	280.7	−163	76	−614	80	23	90	1154	95
Logrono	42.5	357.5	−96	95	−334	101	−73	79	−196	84
Tashkent	41.4	69.2	52	164	−289	164	−138	94	−672	94
Istanbul	41.0	29.1	46	61	−830	66	46	64	−26	69
Fredericksburg	38.2	282.6	72	100	−1078	106	38	52	95	54
Kakioka	36.2	140.2	324	67	−483	70	−113	40	−260	42
Ksara	33.8	35.9	296	63	−643	66	−188	64	−13	67
Tucson	32.2	249.2	287	64	−518	68	69	44	−521	47
Kanoya	31.4	130.9	321	83	−447	90	−150	16	−237	17
Honolulu	21.3	201.0	57	89	−298	92	−148	36	−577	37
Alibag	18.6	72.9	−235	138	−170	146	−200	105	−1188	110
San Juan	18.4	293.9	151	74	−364	78	−85	43	−375	45
M'Bour	14.4	343.0	217	71	−285	74	40	36	−389	38
Muntinlupa	14.4	121.0	138	75	−271	79	270	142	−573	149
Guam	13.6	144.9	225	98	174	105	−23	55	−580	58
Annamalainagar	11.4	79.7	−594	200	219	200	207	53	31	53
Addis Ababa	9.0	38.8	−565	124	101	134	–	–	–	–
Trivandrum	8.5	77.0	−661	82	−262	82	234	100	−391	100
Paramaribo	5.8	304.8	181	113	−325	122	−124	39	−547	43
Bangui	4.4	18.6	−108	86	326	88	446	44	−598	45
Fanning Is.	3.9	200.6	−97	203	363	203	349	84	−720	84
Moca	3.3	8.7	386	130	354	130	−136	25	−673	25
Jarvis Is.	0.4	200.0	128	239	651	239	−4	177	−1265	177
Tatuoca	−1.2	311.5	145	85	42	85	166	51	−1005	53
Lwiro	−2.2	28.8	180	100	571	112	−27	38	−538	42
Hollandia	−2.6	140.5	129	96	988	102	293	29	−729	31

Table 2—*continued*

Station	Latitude (deg)	E. longitude (deg)	H *a*		H *b*		Z *a*		Z *b*	
Huancayo	−12.0	284.7	−198 ±	82	296 ±	86	86 ±	24	−716 ±	25
Apia	−13.8	188.2	163	80	1094	84	79	17	−20	18
Tananarive	−18.9	47.6	−318	66	838	70	216	97	−335	102
Watheroo	−30.3	115.9	−50	71	1096	85	−224	84	−242	100
Hermanus	−34.4	19.2	−224	55	982	58	57	36	106	38
Toolangi	−37.5	145.5	−70	74	823	74	208	38	427	38
Amberley	−43.2	172.7	194	79	1279	83	−84	96	555	101
Trelew	−43.2	294.7	−196	71	1607	73	178	87	51	90
Wilkes	−66.2	110.6	−1090	149	−204	149	1763	812	159	812
Oasis	−66.3	100.7	−530	232	−1120	232	−795	219	1811	219
Mirny	−66.6	93.0	−795	62	1251	73	1292	109	−1910	130
Little America	−78.2	197.8	57	290	1319	290	1010	255	1234	255
Byrd	−80.0	240.0	1184	257	2879	274	−297	291	1435	310
South Pole	−90.0	—	−101	200	3769	238	−997	164	3492	196

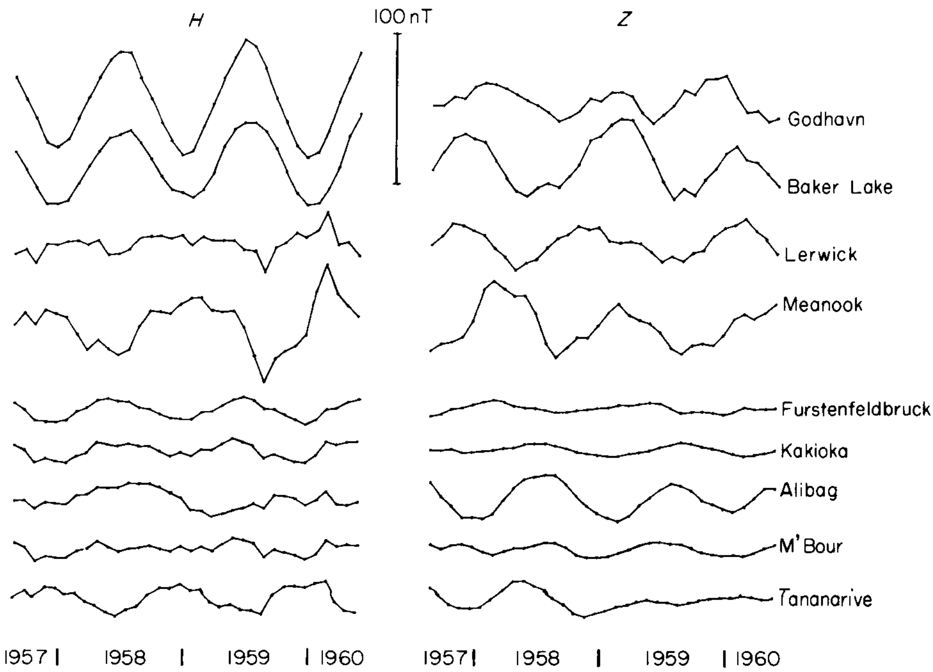

Figure 2. Filtered monthly means for a representative selection of observatories.

a and *b* plotted against dip-latitude, ϕ, where $2 \tan \phi = \tan I$, and I denotes the local value of dip. The most remarkable feature is the large and apparently erratic fluctuation of *a* and *b* at high latitudes. The error bars, representing ±1 sd, indicate that only a small part of this behaviour can be ascribed to the increase in noise towards the poles. These features appear to be unconnected with the behaviour of A_1 over the remainder of the globe, and are certainly not suitable for representation with a low-order spherical harmonic model. The remainder of this section will be concerned with results from dip-latitudes lower than ±60° (representing more than 85 per cent of the Earth's surface); the high latitude effects will be discussed in Section 4.

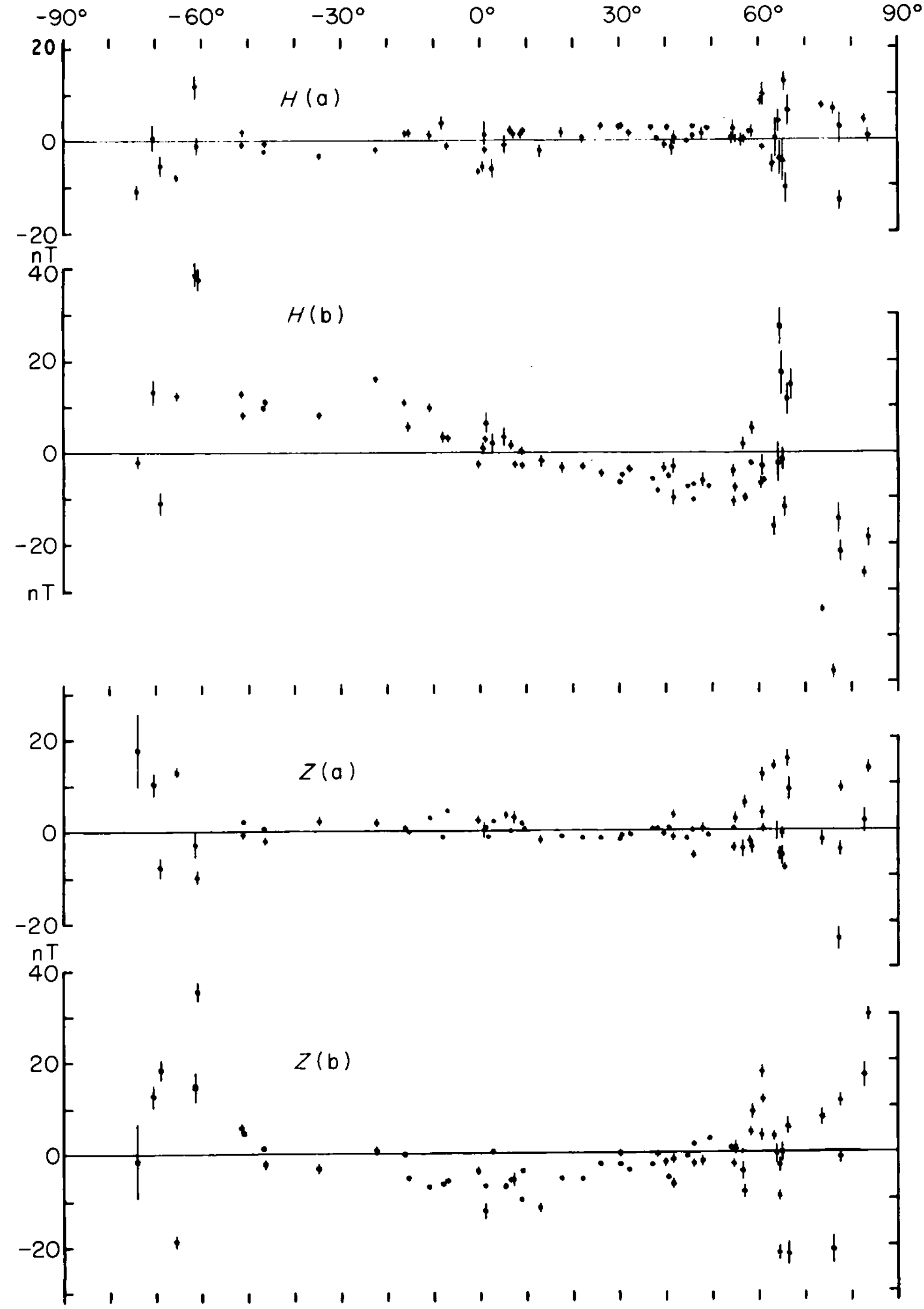

Figure 3. Harmonic constants of the annual variation plotted against dip latitude. The vertical bars indicate ± 1 sd.

Returning to Fig. 3, we note that a, the coefficient of sin t, is well approximated by the zero line, indicating that A_1 is small at the equinoxes. For H, b is negative in the north and positive in the south, showing that H is depressed in winter and enhanced in summer. For Z, b is negative for middle latitudes. These distributions are consistent with A_1 resulting from a P_2^0 term in the magnetic potential.

The most convenient way of separating A_1 into parts of internal and external origin is *via* a spherical harmonic representation. For a satisfactory model, it is important to include all the significant harmonics and exclude all those that are not significant, as has been emphasized by Anderssen (1969). We have already seen that P_2^0 is the dominent term, but others may also be present. Also, to make the best use of the available data, every observation should be included in the analysis, weighted according to its reliability.

The method of analysis closely parallels that detailed by Malin (1973), except that here we have data referring to H, not X and Y. Such non-orthogonal data may be analysed, without loss of rigour, as described by Barraclough *et al.* (1975) in their section on secular variation. After a series of preliminary analyses, it was found that only three harmonic coefficients, g_1^0, g_2^0, g_2^1, could be reliably determined, and that these harmonics were stable, i.e. their numerical values did not change markedly when other harmonics were included in the analysis. The final values of these harmonics for a, b; H, Z, determined from analyses that excluded all other harmonics, are given with their standard deviations in Table 3. Also given in Table 3 are the same spherical harmonic coefficients separated into parts of internal and external origin. Schmidt quasi-normalization has been used throughout.

Table 3. Spherical harmonic coefficients of A_1 in units of 0.01 nT.

	H		Z		Internal		External	
	a	b	a	b	a	b	a	b
g_1^0	−16±41	−347±53	77±24	208±40	46±21	23±32	−62±32	−370±44
g_2^0	−105 26	643 33	33 21	−349 33	−22 16	48 24	−83 20	595 28
g_2^1	66 42	156 55	−9 15	−46 24	21 19	35 26	45 27	121 36

As expected, the external part greatly exceeds the internal part for all three harmonics. The weighted mean ratio of internal to external amplitude is 0.105±0.032, and the weighted mean phase-difference between the internal and external parts is −41°±22° which does not differ significantly from zero.

The major part of A_1 is accounted for by the g_2^0 term, in accordance with the findings of previous investigators. However, we do not agree with their interpretation of this term as resulting from dynamo action in the ionosphere. We consider that a more likely cause is a northward and southward movement of the mean position of the ring-current with a period of one year, for reasons that will be given in Section 5. In addition to the g_2^0 term, there is an appreciable g_1^0 term in the A_1 variation, here determined for the first time. In common with the g_1^0 term found for most of the other geomagnetic variations, it seems probable that this results from enhancement and diminution of the intensity of the ring-current. The only other significant coefficient is g_2^1, which we interpret as a modulation of the g_2^0 term due to the angle between the magnetic axis (which controls the orientation of the ring-current) and the geographic axis (on which the coordinate system is based).

4 Annual variation at high latitude

Results from stations at dip-latitudes greater than ±60° were deliberately omitted from the global analysis of the preceding section because of their large, but localized amplitudes.

Although the high latitude effect appears to be separate from the global phenomenon, it is not reasonable to assume that the reverse is true. If we are correct in interpreting the global effect as due to the ring-current, we would expect this effect to be superimposed on any specifically high latitude effect. Accordingly, in this section we consider the residual annual variation, after removal of that deduced from the global model.

The northern residuals are plotted in Fig. 4 as vectors, with *a* positive to the right and *b* positive upwards. The foot of each vector indicates the invariant latitude, Λ_0, of the observatory. (Invariant latitude is used, since this is the most appropriate for studying particle precipitation effects in the polar regions, and also because we failed to make sense of the residuals when plotted against geographical or dip latitude.) As expected, the residuals are usually small south of $\Lambda_0 = 60°$. The midnight part of the auroral oval in times of moderate magnetic activity is at about $\Lambda_0 = 66°$ (Chubb & Hicks 1970), and it is near here that marked changes occur in the residual vectors. For *H*, the vectors point upwards to the south, and downwards to the north of this latitude. The *Z* residuals are generally upwards except for a narrow band of large downward vectors near 66°.

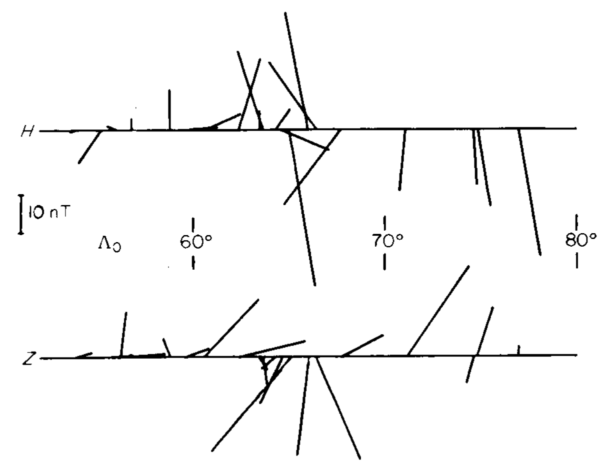

Figure 4. Vector residuals of the high latitude variation from the global model, plotted against invariant latitude.

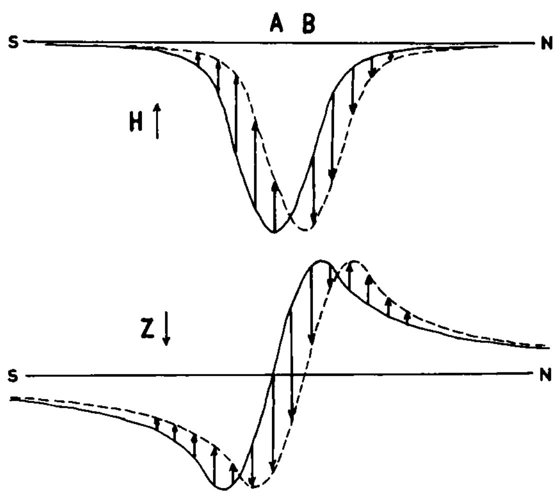

Figure 5. Latitudinal distribution of the magnetic field components due to an east–west current at *A* (solid curve) and *B* (broken curve).

This pattern of behaviour may be interpreted as an annual variation in the mean position of the auroral electrojet (which flows westwards in the ionosphere above the night-time section of the auroral oval), reaching its maximum north latitude in northern winter (December) and its minimum in northern summer (June). This is illustrated in Fig. 5 which shows the latitudinal variation of the vertical and horizontal magnetic fields that would be produced by a current flowing into the page at latitudes A (solid curve) and B (broken curve), representing the summer and winter positions of the auroral electrojet, respectively. The change from summer to winter is indicated by the arrows, and it may be seen that their distribution is broadly similar to that of the vectors in Fig. 4. A more accurate fit could be obtained by varying the parameters of the current (height, width, annual movement, etc.), but the data are too uncertain and the model too crude to justify such an exercise.

The south polar stations are too few to reveal any clear pattern, but the residual vectors are again consistent with a northward movement of the auroral electrojet in December and a southward movement in June.

5 Discussion and conclusions

From a study of the worldwide distribution of the annual variation, we conclude that there are two separate effects present, one global and the other confined to the polar regions.

Previous authors have considered the global effect to result from currents generated by dynamo action in the ionosphere. The strength of such currents would vary directly as the ionospheric conductivity, which diminishes to a small fraction of its daytime value during the night. We have shown in Section 2 that there is no such diminution in the annual variation at night, and hence conclude that it does not originate in the ionosphere. Of the alternative possibilities, neither the direct effect of magnetospheric compression nor the magnetic field of the Sun would be expected to contribute more than a fraction of 1 nT to A_1, and we consider the most likely source to be the ring-current. To reproduce the observed global variation, the mean latitude of the ring-current would need to move north in winter and south in summer (the situation is similar to that illustrated in Fig. 5, though the current is more diffuse and it is no longer valid to ignore the curvature of the Earth). We suggest that such a north–south motion may result from the compression of the Earth's magnetic field by the solar wind. The field is distorted by being compressed on the side towards the Sun, and expanded on the side away from the Sun. In particular, the lines of force that define the geometry of the ring-current are displaced away from the Sun. During northern winter, the south pole is inclined towards the Sun, and hence the ring-current is displaced to the north; the reverse applies in northern summer; this is illustrated in Fig. 6.

Superficially, the polar effect is rather similar, though its amplitude is much greater and its distribution more localized than the global effect. However, the extremely rapid variation with latitude of the polar effect argues against an origin at any great altitude, and its close correlation with the auroral oval strongly suggests that it results from the auroral electrojet. The observed polar effect appears to result from a northward and southward movement of the electrojet in December and June, respectively. It is not immediately obvious why this should occur, but it is probably related to the fact that, in December, the higher latitudes are inclined towards the neutral sheet in the magnetotail, which is the source of the particles which flow in the electrojet.

A more detailed study would be required to further elucidate the polar effect, with the annual variation determined from data for each hour of local time. It would also be of interest to make a detailed study of the variation of A_1 with the solar cycle.

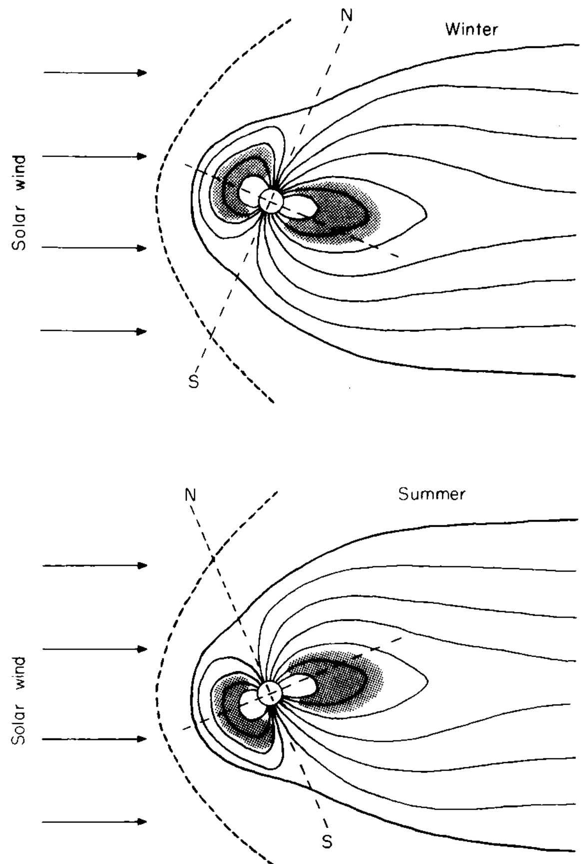

Figure 6. Schematic diagram to illustrate how the ring current (shaded area) may be moved north in winter and south in summer by the solar wind (arrows).

Acknowledgments

This work was carried out at the Institute of Geological Sciences while one of us (AMI) was supported by a grant from the Scientific and Technical Research Council of Turkey. Many of the data used here were provided by World Digital Data Centre C1.

References

Anderssen, R. S., 1969. *J. geophys. Res.*, **74**, 1045.
Banks, R. J., 1969. *Geophys. J. R. astr. Soc.*, **17**, 457.
Banks, R. J., 1972. *J. geomagn. geoelect., Kyoto*, **24**, 337.
Barraclough, D. R., Harwood, J. M., Leaton, B. R. & Malin, S. R. C., 1975. *Geophys. J. R. astr. Soc.*, **43**, 645.
Chubb, T. A. & Hicks, G. T., 1970. *J. geophys. Res.*, **75**, 1290.
Currie, R. G., 1966. *J. geophys. Res.*, **71**, 4579.
Currie, R. G., 1974. *J. geomagn. geoelect., Kyoto*, **26**, 319.
Cynk, B., 1939. *Terr. Mag. atmos. Elect.*, **44**, 51.
Gupta, J. C. & Malin, S. R. C., 1972. *Geophys. J. R. astr. Soc.*, **30**, 11.
Leaton, B. R., Malin, S. R. C. & Finch, H. F., 1962. *R. Obs. Bull.*, **63**.
Lloyd, H., 1874. *A treatise on magnetism, general and terrestrial*, Longmans, Green & Co., London.

McIntosh, D. H., 1959. *Phil. Trans. R. Soc. Lond. A.*, **251**, 525.
Malin, S. R. C., 1973. *Phil. Trans. R. Soc. Lond. A.*, **274**, 551.
Schwalbe, G., 1898. *Meteorol. Z.*, **15**, 449.
Schwalbe, G., 1899. *Meteorol. Z.*, **16**, 325.
van Wijk, A. M., 1953. *J. geophys. Res.*, **58**, 418.
Vestine, E. H., 1954. *J. geophys. Res.*, **59**, 93.
Vestine, E. H., Lange, I., Laporte, L. & Scott, W. E., 1947. *Carnegie Inst. Washington,* Publ. **580**, 93.